

Shlyk, Sergii

## Article

# Research of ANSYS Autodyn capabilities in evaluating the landmine blast resistance of specialized armored vehicles

**Reference:** Shlyk, Sergii (2021). Research of ANSYS Autodyn capabilities in evaluating the landmine blast resistance of specialized armored vehicles. In: Technology audit and production reserves 3 (1/59), S. 6 - 15.

<http://journals.uran.ua/tarp/article/download/235397/234377/539551>.

doi:10.15587/2706-5448.2021.235397.

This Version is available at:

<http://hdl.handle.net/11159/7016>

## Kontakt/Contact

ZBW – Leibniz-Informationszentrum Wirtschaft/Leibniz Information Centre for Economics  
Düsternbrooker Weg 120  
24105 Kiel (Germany)  
E-Mail: [rights\[at\]zbw.eu](mailto:rights[at]zbw.eu)  
<https://www.zbw.eu/econis-archiv/>

## Standard-Nutzungsbedingungen:

Dieses Dokument darf zu eigenen wissenschaftlichen Zwecken und zum Privatgebrauch gespeichert und kopiert werden. Sie dürfen dieses Dokument nicht für öffentliche oder kommerzielle Zwecke vervielfältigen, öffentlich ausstellen, aufführen, vertreiben oder anderweitig nutzen. Sofern für das Dokument eine Open-Content-Lizenz verwendet wurde, so gelten abweichend von diesen Nutzungsbedingungen die in der Lizenz gewährten Nutzungsrechte.

<https://zbw.eu/econis-archiv/terms-of-use>

## Terms of use:

*This document may be saved and copied for your personal and scholarly purposes. You are not to copy it for public or commercial purposes, to exhibit the document in public, to perform, distribute or otherwise use the document in public. If the document is made available under a Creative Commons Licence you may exercise further usage rights as specified in the licence.*



Sergii Shlyk

# RESEARCH OF ANSYS AUTODYN CAPABILITIES IN EVALUATING THE LANDMINE BLAST RESISTANCE OF SPECIALIZED ARMORED VEHICLES

*The object of research is the processes of pulse explosive loading in an explicit formulation for simulation of complex nonlinear dynamics of solids, gases, and their interactions. One of the most problematic areas of modern studies of nonlinear dynamic loads of materials using a numerical analysis is that such studies usually do not take into account the characteristic transition of the stationary deformation zone of the loaded material to the unsteady one and the front pressure and shockwave velocity variation by time.*

*The work is aimed at developing a mathematical model of a pulsed load of materials by a shockwave, developing a mathematical apparatus for calculating the parameters of a shockwave, creating analytical dependences of the interaction of a shockwave with a loaded surface. A study of dynamic explosive loading using software based on an explicit method for solving the equations of continuum mechanics is proposed.*

*In this work, the stress-state equation at a point of the material under pulsed load conditions was further developed, methods for determining the principal stresses and the invariant of the stress tensor, taking into account the pulsed nature of the load, were established. The character of the behavior of the shockwave formed as a result of the detonation of the explosive has been established. Analytical dependences of the interaction of a shockwave with a loaded surface are compiled. A mathematical apparatus has been developed for calculating such parameters of the shockwave as the detonation front pressure and its change in time and the velocity of the shockwave at the moment when it reaches the surface.*

*Mathematical dependences have been developed and proposed, which, in contrast to the existing ones, make it possible to determine the current values of stresses and strains passing through the points of the actual stress curve, as well as the intensity of stresses and strains under pulse loading of metals.*

*On the basis of theoretical and experimental studies of the parameters of body material deformation under the action of explosive loading, the mechanisms of destruction of the KrAZ «Shrek» and KrAZ «Fiona» (Ukraine) specialized armored vehicles body were clarified to establish the compliance of the declared landmine resistance of vehicles with the STANAG 4569 standardization agreement.*

**Keywords:** anti-vehicle mines, pulse explosive loading, armored vehicles, mathematical model of deformation, finite element method.

Received date: 15.01.2021

Accepted date: 23.02.2021

Published date: 30.06.2021

© The Author(s) 2021

This is an open access article

under the Creative Commons CC BY license

## How to cite

Shlyk, S. (2021). Research of ansys autodyn capabilities in evaluating the landmine blast resistance of specialized armored vehicles. *Technology Audit and Production Reserves*, 3 (1 (59)), 6–15. doi: <http://doi.org/10.15587/2706-5448.2021.235397>

## 1. Introduction

According to the United Nations Office for the Coordination of Humanitarian Affairs (OCHA), the Convention on the Prohibition of the Use, Stockpiling, Production and Transfer of Anti-Personnel Mines and on their Destruction since 1997 did not reduce their global application, as it is estimated that more than 100 million mines are installed in 60 countries around the world. Landmines (including anti-vehicle) are also widely used in modern conflicts [1]. To date, the actual standard for armored military vehicles is the compliance of the MRAP class (Mine Resistant Ambush Protected). The NATO STANAG 4569 standardization

agreement defines necessary to class MRAP vehicles crew protection in case of landmine blast action (charge weight is 6 kg in TNT equivalent) under any of the wheels or tracks and under the hull center [2].

Finite element analysis (FEA) is widely used in research related to defense industries, such as high-speed collision and penetration. Numerical simulation of processes allows to obtain additional information on complex physical phenomena, which is not available in experimental research methods. ANSYS Autodyn is an analytical tool for solving problems in explicit statement for simulation of complex nonlinear dynamics of solids, liquids, gases and their interaction. It represents a powerful tool for

interdisciplinary calculations in problems with explicit statement, which provides a wide range of possibilities for simulation, including high-speed strikes or explosion [3].

Despite the high degree of reliability of the achieved simulation results, each specific case of simulation is a solution to a particular problem that requires reliable experimental confirmation. There is no universal method for solving problems that do not require lengthy and painstaking preparatory work. Therefore, it is relevant to conduct research related to expanding the capabilities of existing software systems for simulating a pulsed explosive loading of modern specialized vehicles.

## 2. The object of research and its technological audit

*The object of research* is the processes of pulse explosive loading in an explicit formulation for simulation of complex nonlinear dynamics of solids, gases, and their interactions associated with the transition from a stationary deformation zone to a nonstationary one with force intensification.

According to a study by the Geneva International Center for Humanitarian Demining (GICHD), 169 incidents involving the detonation of anti-vehicle mines (AVM) were recorded worldwide. The number of victims of AVMs worldwide was 487 people (15 % increase compared with 2016) – 321 were injured, 166 were killed. Across 24 states and territories where such incidents were recorded 51 % of casualties were civilians. Ukraine, Pakistan, Mali and Iran were the four states with the most recorded AVM incidents in 2017, followed by Chad, Syria, Western Sahara and Yemen. Since 2015, Ukraine has been the state with most recorded incidents for three consecutive years, and Mali has continuously featured among the top three affected states [1]. The Center estimates that each year of war in any conflict is a further 10 years for demining conflict areas. For example, according to the UN Office for the Coordination of Humanitarian Affairs, only in Ukraine the territory «contaminated» by mines covers an area of 300 square kilometers.

For these reasons, the mine protection function is a prerequisite for combat vehicles, armored personnel carriers, and other vehicles operated in combat conflict zones.

KrAZ «Shrek» and KrAZ «Fiona» (Fig. 1) are the family of Ukrainian armored vehicles with V-hull developed by PJSC «AutoKrAZ» (Ukraine) in cooperation with STREIT Group (United Arab Emirates) on the basis of KrAZ-5233BE. The vehicles are developed in accordance to the MRAP standard and presented in 2014. The vehicles are intended for the prompt deliverance of the military units' personnel and their fire support. In addition, they can be used as a various weapons and military equipment carriers.

Mine protection of MRAP class vehicles is provided by the V-shaped (wedge-shaped) form of the lower part of the body, the increased durability of the bottom, and the application of energy-absorbing seats. The purpose of the armored bodies with a V-shaped bottom is to increase mine resistance and increase the survival of the crew on the battlefield by deflecting in the lateral direction of high explosive (pulse pressure of explosive products) when detonating under the hull of mines or improvised explosive devices (IED). This solution, in addition to the redistribu-

bution of the released energy of the explosion, provides an increase in ground clearance and bottom height (floor of the combat and landing department).



a



b

**Fig. 1.** General view of the multi-purpose vehicles:  
a – KrAZ «Shrek»; b – KrAZ «Fiona»

AUTODYN has proven itself well in the tasks of ballistic loading of materials. Modeling the behavior of such materials is impossible without taking into account the complex anisotropic elastic-plastic nature of the behavior, the nonlinear nature of the shockwave compression, as well as the anisotropic fracture with the effects of progressive softening. AUTODYN's capabilities for combining hydrodynamic and strength solvers also allow it to simulate a combination of explosive and debris effects on structures.

This study provides a theoretical assessment by modeling the landmine protection of the body of KrAZ «Shrek» and KrAZ «Fiona» armored vehicles when detonating an explosive weighing 6, 8, 10, 14, and 20 kgs in TNT equivalent. Three cases are considered: blasting under the front wheel, rear wheel, and under the center of the vehicle. Mine resistance assessment was performed in accordance with the NATO AEP-55 STANAG 4569 standard.

The assessment of the anti-vehicle mines blast resistance was carried out by the finite element method (FEM) simulation. The calculation system includes atmospheric air, a simplified model of the vehicle body (Fig. 2), explosive charge, and soil mass. Locations of charge relative to the body in the model are shown on Fig. 3.

To date, studies of mine protection and other nonlinear dynamic loads (small arms damage, etc.) of vehicles by numerical analysis have focused mainly on the structural deformations of the studied models. Usually, the parameters of the environment (air, soil, etc.) are not taken into account in the calculations. Further development of such studies is, among other things, soil modeling, as experimental studies show that different types of saturated soils with high moisture significantly affect the characteristics of shockwaves, especially in deeply laying landmines.

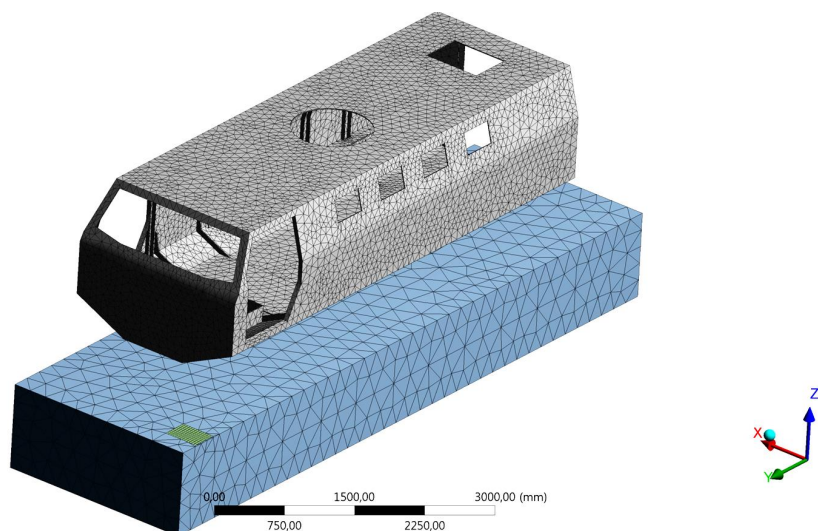


**Fig. 2.** General view of the finite-element model (the explosive charge is located under the vehicle left front wheel; atmospheric air is not shown)

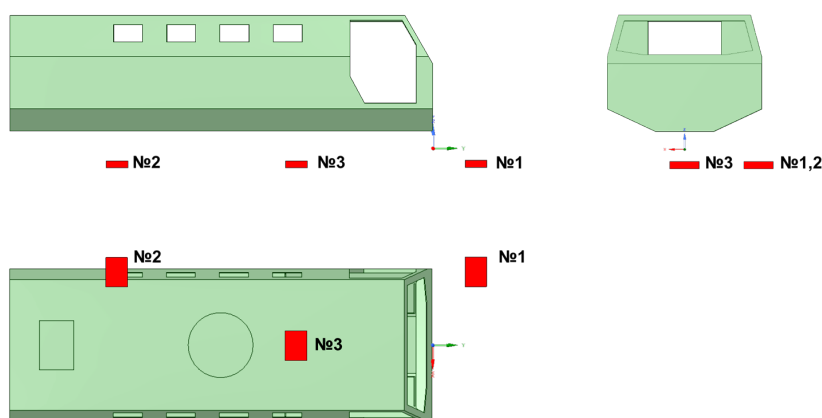


**Fig. 3.** Location of the explosive charge during the simulation:  
1 – under the left front wheel; 2 – under the left rear wheel; 3 – under the vehicle center

AUTODYN has its own library of materials, but the soil model presented in the library is incomplete and presented in the form of several «pure» materials, such as sand, clay, etc., and therefore is insufficient to model the full interaction of the shockwave and its subsequent reflection on the body and into the environment. Trinitrotoluene (TNT) is present in the library, however, according to documented data from the software manufacturer, it is presented as a standard measure of explosive power, so it needs to detail certain parameters, and body material, Quardian 500 armor steel, is missing in the library. Therefore, when compiling a mathematical model of the process of explosive loading of the body, the possibilities of creating and modifying materials available in the AUTODYN library were used.

### 3. The aim and objectives of research

The aim of research is a theoretical assessment of the structural strength of the specialized vehicles KrAZ «Shrek» and KrAZ «Fiona» armored body to the explosive load caused by blast of explosive with mass 6, 8, 10, 14 and 20 kg in TNT equivalent. To achieve this aim it is necessary to perform the following objectives:

1. To investigate the nature of the behavior of the shock wave formed as a result of the detonation of an explosive.

2. To perform the theoretical calculation of mine resistance of KrAZ «Shrek» and KrAZ «Fiona» MPVs bodies according to the requirements of the NATO AEP-55 STANAG 4569 standardization agreement.

3. To confirm to the KrAZ «Shrek» and KrAZ «Fiona» MPVs body landmine resistance according to the requirements of STANAG 4569 levels.

4. To investigate the mechanism of the KrAZ «Shrek» and KrAZ «Fiona» MPVs body destruction under pulse explosive loading in case of the estimated destruction.

### 4. Research of existing solutions to the problem

In the work [4] it was made a look at the near-field explosion in soil by using numerical techniques. It was investigated that numerical techniques are cost-effective and easier to set up and run (when compared with experiments). And that numerical simulation can recreate scenarios and physical parameters and allow flexibility in a way experiments cannot. A framework for deriving the model for soil with varying moisture contents was proposed. The subject of the study was prairie soil (cohesive soil). Standard soil laboratory data are used to determine soil properties that are then used to define a numerical soil model.

In [5, 6] blast-induced dynamic fractures were studied under highly controlled conditions. The whole cycle of conducting a series of the laboratory-scale blast, analyzing the results, and using them to test the validity of an advanced numerical code is reported in these works.

In the work [7] were investigated that in order to determine the loads on mine-clearing devices generated by detonations of anti-tank mines, knowledge about the incident impulse and pressure generated in the air is needed. Determined that dependent factors include the mine's depth of burial and the properties of the soil. Numerical simulations were performed with a multi-material Euler processor to determine incident impulses and pressure histories from detonations of fully buried, flushed, and surface anti-tank mines for dry porous sand and saturated clay. At the same time, the works [8, 9] were established that the numerical simulation of penetration into sand is one of the most challenging problems in computational geomechanics. The papers present an arbitrary Lagrangian-Eulerian (ALE) finite element method for plane and axisymmetric quasi-static penetration into sand which overcomes the problems associated with the classical approaches. An operator-split is applied which breaks up a solution of the governing equations over a time step into a Lagrangian step, a mesh motion step, and a transport step. A unique feature of the ALE method is an advanced hypoplastic rate constitutive equation to realistically predict stress and density changes within the material even at large deformations.

In papers [10, 11] is proved that in the blast phenomena, the interaction between fluid and structure, also called



fluid-structure interaction (FSI), normally will occur, and there is no single method that can be used for all conditions in FSI analysis. The governing partial differential equation for the FSI model needs to be solved in both time and space domain with the basic physic principles involving the conservation of mass, momentum, and energy. It is proved that the solution over the time domain can be achieved by an explicit method. It can be obtained by utilizing different spatial discretization such as Lagrange, Euler, and Arbitrary Lagrangian-Eulerian (ALE) or mesh-free method also known as Smooth Particle Hydrodynamic (SPH) methods. However, the basic solvers for explicit integration numerical wave-codes (sometimes termed «hydro-codes») can be utilized as an outline with their associated strengths and weaknesses. Air, plate, and trinitrotoluene (TNT) are three different domains in the model analysis. In addition, the paper [11] presents the appropriate solver coupling of a rolled homogeneous armor (RHA) plate subjected to blast loading and has been compared with [12] experimental data. For this case, it was found out that using the ALE solver to represent both the TNT and RHA plate in the numerical simulation, managed to produce a good agreement with the experimental test data. Thus, the ALE solver will be chosen as the coupling solver to simulate similar cases for future analysis.

Thus, it has been established that blast modeling and simulation is a very important field in the military land vehicle industry. Increasing demands for higher protection levels lead the engineers to more challenging design and simulation cases. In most situations, Arbitrary Lagrange Euler (ALE) method is the most well-known method for blast simulations and also for determining the effects of blast loads on structures.

It should be noted that in the listed works much attention is paid to the development of mathematical models of a blast shock wave, as well as impulse loading of soils and materials. For example, an efficient optimization-based algorithm has been implemented to smooth out the non-convexly distorted mesh regions. At the same time, works in which the problem of simultaneous linking of the solution of these problems would be solved are absent or require clarification. Only sand with different moisture content, clay, or rocks are considered as geological materials subject in studies of explosive loading, and the models of materials do not take into account their hardening and force intensification of the process. Due to the complex response of soil under high impulse loading and thermodynamic behavior of detonation products, perhaps the most significant source of modeling error lies in the constitutive treatment of these materials. Therefore, in simulating near-field blast events, it is critical that representative material models are available for the problem under consideration.

The numerical techniques using the spatial discretization scheme that has been provided as a solver in the AUTODYN computer code are used in different studies in order to predict the armor response subjected to explosive (TNT) blast loading. The final deflection is usually used as a reference in order to identify the suitable solver for both materials of armor and TNT. Only then the plastic deformation will be chosen in the simulation process. Instead of using the same solver for vehicles body material and TNT, the optimization of the solver can be achieved if it is only used in an appropriate domain, or in other words, a different domain will be using a different solver.

The solvers, which were available in AUTODYN, should be used in the analysis of impact and explosion or fluid-structure interaction. Therefore, in this paper, let's determine the suitable solver for both materials (TNT and body material), and the appropriate interaction coupling solver will be obtained.

## 5. Methods of research

The process of detonation is numerically described by the general system of differential equations. The materials models play an important role, which relates the deformation stress and internal energy. Liquids and gases (in this study the detonation products and air) are sufficiently modeled by the equation of state (EOS), which expresses the relationship between pressure  $p$ , specific volume  $V$ , and specific energy  $e$ . Additional equations are required for solids simulation (in presented study the body material), since solids possess a shear resistance.

As a soil, in the calculation model, the loess loam is used. It is the loam species, which is characterized by high content of clay particles, the presence of coarse sand and (less) pebble material. To determine the soil model, the data obtained in [4, 5, 13] were used. The model used in this study was obtained for sand with a moisture content of 6.57 % by the three-dimensional compression, which made it possible to measure the velocity of the waves in the sand sample.

The atmospheric air was modeled using the ideal gas EOS. The initial density was  $1.3 \text{ kg/m}^3$  and the internal energy was  $192.31 \text{ kJ/kg}$ , which is equal to an atmospheric pressure of  $100 \text{ kPa}$  (one atmosphere) at  $0^\circ\text{C}$ . In addition, an alternating pressure was given, that allows achieving the zero pressure in the air during the simulation. This makes it possible to avoid unwanted starting velocities [7].

Properties of the applied explosive model (trinitrotoluene) are specified according to [5, 6]. When considering the process of loading and interaction of flat material (plate) with a shockwave formed during the detonation of an explosive, the process is considered as two-stage:

- 1) acquisition of the initial velocity at the passage of the shockwave on the surface and its output on the free surface;
- 2) further acceleration of the plate under the pressure of detonation products of the explosive.

The material of the plate is divided into elements with a mass concentrated in one point of reduction. Those elements are interconnected by elastic-plastic joints. The plate elements equation of motion under the action of detonation products pressure can be written in the form:

$$Dm \frac{d^2 x_1(t)}{dt^2} + \rho c \frac{dx_1(t)}{dt} = P(t), \quad (1)$$

where  $m$  – mass of the element of the plate square unit;  $dx_1/dt$  – velocity of the plate in the direction of displacement;  $\rho_1, c$  – density and sound speed in the environment behind the plate;  $P(t)$  – pressure, which describes the detonation products action on the plate.

The detonation front pressure changes according to the law:

$$P(t) = P_0 \exp(-t / \theta), \quad (2)$$

where  $P_0$  – pressure of the detonation products on the plate at the moment of the shockwave release onto the free surface;

$\theta$  – time constant for the decline of detonation products;  
 $t$  – time of the process.

The solution of (1) when neglecting the second term has the form:

$$\dot{x}_1(t) = \frac{P_0 \theta}{m} (1 - \exp(-t/\theta)) + v_0, \quad (3)$$

where  $v_0$  – initial velocity of the plate element at the moment of the shockwave release to the free boundary.

To determine  $P_0$  and  $\dot{x}_0$  the Chapman-Jouguet condition [10, 14] for the pressure at the detonation front is used:

$$P_n = \rho_0 D^2 / (k+1), \quad (4)$$

where  $\rho_0$  – initial density of the explosive;  $D$  – detonation velocity of the explosive;  $k$  – indicator of the explosive adiabatic.

The pressure on the plate to the pressure of the detonation products ratio is determining by the equation:

$$P_x / P_n = [0.5(3k-1)k^{-1}]^{2k/(k-1)}. \quad (5)$$

At the moment of the shockwave release to the free surface, the pressure of the detonation products on the plate is determined by the expression:

$$P_x = [0.5(3k-1)k^{-1}]^{2k/(k-1)} P_n [H \cdot D^{-1} (H/D + t_0)], \quad (6)$$

where  $t_0 = \delta_M / c_M$  – time of a shockwave passing on a plate;  $c_M$  – shockwave velocity in the plate;  $\delta_M$  – plate thickness;

$$c_M = a + \lambda u_x, \quad (7)$$

where  $u_x$  – mass velocity of the plate;  $a$  – soundspeed;  $\lambda$  – shock compression coefficient of the plate material.

The shockwave velocity at the moment of release on the plate free surface is determined by the ratio:

$$c_M = P_0 \cdot (\rho_M \cdot u_x)^{-1}. \quad (8)$$

The system of equations for calculating  $P_x$ ,  $u_x$  and  $c_M$  at the moment of the shockwave release on the plate free surface has the form:

$$\begin{cases} P_x = [0.5(3k-1) \cdot k^{-1}]^{2k/(k-1)} P [H \cdot D^{-1} (H/D + t_0)^{-1}]^k, \\ c_M = a + \lambda u_x, \\ t_0 = \delta_M / (a + \lambda u_x), \\ P_x = \rho_M u_x \cdot c_M. \end{cases} \quad (9)$$

At the explosive charge blast, the maximum pressure at the front of the shockwave is determined by the empirical formula [10, 15]:

$$P_m = \frac{1.08}{(r_0)^{1.08}} \cdot 10^4, \quad (0.0773 \cdot 10^{-4} \leq r \leq 1.082 \cdot 10^{-4}), \quad (10)$$

where  $r_0 = r / \sqrt{q}$  – reduced explosion distance;  $r$  – explosion distance, m;  $q$  – explosion energy per length unit, J/m.

The change in pressure, depending on the location of the shockwave front point, is approximated by the dependence:

$$P_m = (31.14 + 89.86\lambda + 380.69\lambda^2) \cdot 10^5, \quad (11)$$

where  $\lambda$  – length of the arc along the shockwave front from a given front point assigned to the length of the arc from the axis of charge to the front point equidistant from both ends.

According to the foregoing, the field of the shockwave peak pressures can be described with sufficient accuracy by expression:

$$P_m = 0.1241 \cdot 10^7 \left( \frac{q}{q_0} \right)^{0.572} \cdot r^{-1.144} + \left[ 0.1166 \cdot 10^8 \cdot \left( \frac{q}{q_0} \right)^{0.4} \cdot r^{-0.805} - 0.1241 \cdot 10^7 \left( \frac{q}{q_0} \right)^{0.572} \cdot r^{-1.144} \right] \cdot \lambda. \quad (12)$$

The body of the vehicles is the integral type body of supporting structure, which is assembled from 8 mm steel armored plates of Quardian 500. Quardian 500 is protective sheet steel that combining high properties of ballistic resistance with high strength and an average Brinell hardness of 500 HBW. It is used in the public sphere (protection of embassies, government and public buildings, banking institutions), special protection, and military applications (armoring of helicopters, boats, demolition vehicles and armored personnel carriers). The main characteristics of Quardian 500 steel are given in Table 1.

Table 1

Mechanical properties of the steel Quardian 500

| Hardness, Brinell | Impact strength (cutting, -40 °C (min.)), J·m <sup>-3</sup> | Yield stress, MPa | Ultimate tensile strength, MPa | Elongation A50, % |
|-------------------|---|-------------------|--------------------------------|-------------------|
| 480–540           | 24  | 1200              | 1450–1800                      | 8                 |

Considering a flat vehicles body surface let's cover it with the spatial Lagrangian mesh, which is associated with the median surface, and use the «node scheme», in which all the required quantities are determined at the nodal points of the calculated grid. It should be noted that with such a construction of the difference scheme, the second derivatives with respect to the spatial coordinates are approximating satisfactorily. In conditions of complex loading, the process of forming is associated with the transition from a stationary deformation to a non-stationary one. In a non-stationary deformation, the change in the Lagrange coordinates of the mesh element during the process of forming is accompanied by a simultaneous change in the deformation cell. As a result, the magnitude of the stresses in the mesh element does not change in the process of deformation. The material is considered as isotropic elastic-plastic with hardening. The mesh acceleration in the median plane, its velocity and displacement is determined from the equilibrium equations for each node [3, 6]:

$$\begin{cases} \nabla_\gamma M_{mn}^{\beta\alpha} - Q_{mn}^\beta R_{pn}^\beta + P_{mn}^\alpha + T_{mn}^\alpha + S_{mn}^\alpha = \bar{\rho} \ddot{X}_{mn}^\alpha - \rho \dot{X}_{mn}^\alpha c, \\ M_{mn}^{\beta\alpha} R_{\beta\alpha}^{mn} + \nabla_\beta Q_{mn}^\beta + P_{mn}^3 + T_{mn}^3 + S_{mn}^3 = \rho \ddot{X}_{mn}^3 - \rho \dot{X}_{mn}^3 c, \\ \nabla_\beta L^{\alpha\beta} - Q_{mn}^\alpha = 0, \end{cases} \quad (13)$$

where  $\nabla_\beta$  – sign of a covariant differentiation;  $M_{mn}$  – membrane forces;  $L$  – bending moments;  $Q_{mn}^\beta$  – cutting forces;

$\bar{\rho}$  – reduced weight;  $\ddot{X}_{mn}^j$  – acceleration;  $P_{mn}^j$  – force effect of loading;  $T_{mn}$  – friction forces in the peripheral zone of the element;  $S_{mn}$  – braking forces of the resistance elements;  $P_{mn}$  – forces acting in the mesh element from the elements of resistance;  $R_{mn}$  – tensor of curvature;  $c$  – soundspeed in the environment.

Taking into account the fact that the process of forming is associated with force intensification it is more appropriate to submit equilibrium equation in the forces and moments as it shown on Fig. 4.

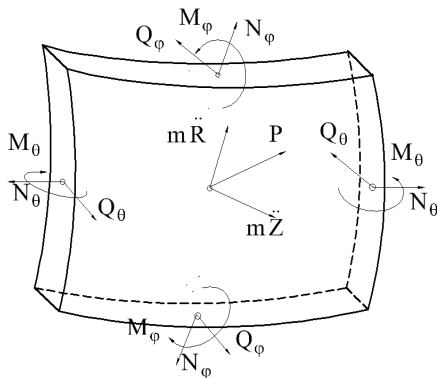


Fig. 4. Forces in the element of the material

The values of forces and moments acting on each element are determined by the system of equations [16]:

$$\begin{cases} M_{mn}^{\alpha\beta} = \int_{-0.5\delta}^{+0.5\delta} \left[ \sigma_{\alpha_1}^{mn} (\delta_1^\beta - x^3 B_{1mn}^\beta) + \right. \\ \left. + \sigma_{\alpha_2}^{mn} (\delta_2^\beta - x^3 B_{2mn}^\beta) \right] (G_{mn} \cdot A_{mn}^1)^{0.5} dx, \\ I_{mn}^{\alpha\beta} = \int \left[ \sigma_{\alpha_1}^{mn} (\delta_1^\beta - x^3 B_{1mn}^\beta) + \right. \\ \left. + \sigma_{\alpha_2}^{mn} (\delta_2^\beta - x^3 B_{2mn}^\beta) \right] \cdot (G_{mn} \cdot A^{-1})^{0.5} x^3 dx, \\ Q_{mn}^\alpha = \frac{\partial I_{mn}^{\alpha\beta}}{\partial x^\beta} + \bar{A}_{mn}^\alpha \cdot \frac{\partial \bar{A}_{mn}^{\alpha\beta}}{\partial x^\beta} \cdot L_{mn}^\beta + \bar{A}_{mn}^\beta \cdot \frac{\partial \bar{A}_{mn}^{\alpha\beta}}{\partial x^\beta} \cdot L_{mn}^\alpha, \end{cases} \quad (14)$$

where  $A_{mn}^{\alpha\beta}$  – metric tensor.

The acceleration of the grid nodes median surface in the next field of integration should be determined by the equation:

$$\begin{aligned} \ddot{X}_{mn}^j = & \frac{A_{mn}^{0.5}}{\bar{\rho}_o} \cdot (P_{mn}^j + T_{mn}^j + S_{mn}^j + \Pi_{mn}^j) + \\ & + \frac{A_{mn}^{0.5}}{\bar{\rho}_o} \cdot \left( \frac{\partial V_{mn}^{\beta j}}{\partial x^\beta} + \bar{A}_{mn}^\beta \cdot \frac{\partial \bar{A}_{mn}^{\alpha\beta}}{\partial x^\beta} \cdot V^{\alpha j} \right), \end{aligned} \quad (15)$$

where  $A_{mn}$  – determinant of the metric tensor;  $V_{mn}^{\alpha j}$  – space-surface tensor.

The time interval  $\Delta t$  is chosen from the stability condition of the computational process [10]:

$$\Delta t \leq \Delta X_{5,j,0} [\rho_3^k (1 - \nu_k)^2 (E)^{-1}]^{0.5}, \quad (16)$$

where  $\rho_3^k$  – density of the body material;  $\nu_k$  – Poisson's ratio;  $E$  – Young's modulus of the body material.

To build the «stress – deformation» diagram that is specified as dependencies in describing of the material in the ANSYS library, the following expressions were obtained:

$$\frac{\partial^2 \sigma_i}{\partial \varepsilon_i^2} = n(n-1) C \varepsilon_i, \quad (17)$$

$$\sigma_2 = \sqrt{\sigma_1 \cdot \sigma_3}, \quad (18)$$

$$\sigma_i = \frac{3}{2} H \varepsilon_i^n / [0.29 - 2D + \ln C_3 (n_c + 0.75 \varepsilon_i^n) \varepsilon_i^n], \quad (19)$$

$$n = \frac{\lg \sigma_3 - \lg \sigma_1}{\lg(\varepsilon_o + \varepsilon_3) - \lg(\varepsilon_o + \varepsilon_1)}, \quad (20)$$

$$C = \frac{\sigma_1}{(\varepsilon_o + \varepsilon_i)^n}, \quad (21)$$

$$\begin{cases} \sigma_i = C (\varepsilon_o + \varepsilon_i)^n, \\ \sigma_1 = C (\varepsilon_o + \varepsilon_1)^n, \\ \sigma_2 = C (\varepsilon_o + \varepsilon_2)^n, \\ \sigma_3 = C (\varepsilon_o + \varepsilon_3)^n, \end{cases} \quad (22)$$

where  $\sigma_1, \sigma_2, \sigma_3, \varepsilon_1, \varepsilon_2, \varepsilon_3$  – current values of stresses and deformations passing through the points of the curve of actual stresses;  $\varepsilon_1, C, n$  – constants which are satisfying the system of equations (22);  $\sigma_3, \varepsilon_1$  – stresses and the strains intensities.

## 6. Research results

**6.1. Experimental results.** An important criterion that determines the validity of the results obtained by the simulation and the adequacy of the developed mathematical model to the real process is the correspondence with the data obtained as a result of experimental tests. For experimental studies, a series of Quardian 500 steel plates of 8 mm thickness and 500×500 mm in size was used. The plates were located in sandy soil (Fig. 5) and subjected to a dynamic load by explosion of Amatol and Ammonium Nitrate mixture with an aggregate capacity of 10 kgs in a TNT equivalent. In order to better explosive load transfer on the Quardian 500 steel plate and the possibility of more accurate deflections recording, a striker plate made from Mangalloy (Hadfield steel) in the size of 125×375 mm and 5 mm thickness was used. The striker plate was located on a test plates under the charges of an explosive. During the experiment, the values of dynamic displacements of the deformed plate were recorded.

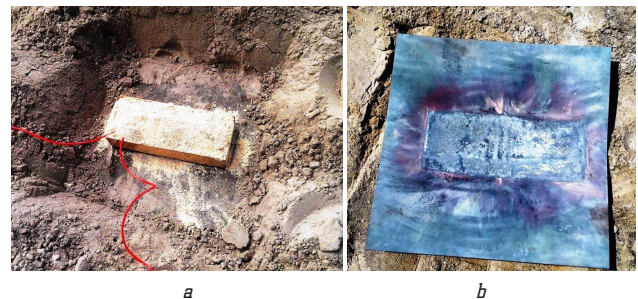
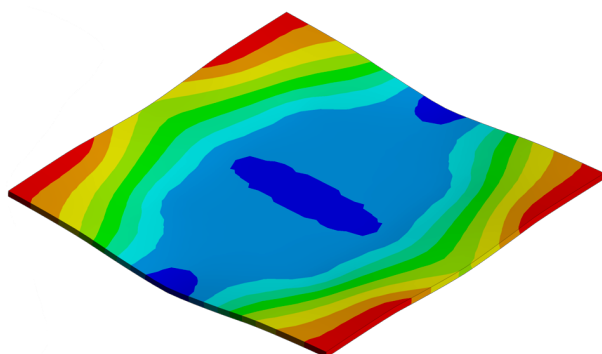


Fig. 5. Experimental study of the Quardian 500 plate dynamic explosive loading; a – the Quardian 500 plate with mounted explosive charge, striker plate and detonator; b – deformation of Quardian 500 plate by blast

In addition, the numerical simulation of the Quardian 500 steel plate explosive loading was performed in the ANSYS Autodyn system using the data, dependencies and assumptions described in Section 2 (Fig. 6).





**Fig. 6.** Deformations diagram of the investigated plate along the Y-axis

The simulation system included the atmospheric air, explosive charge (9.9 kg of TNT), striker plate, Quardian 500 plate and soil. The relative error of the deflection differences values at the control points obtained by the field and numerical experiments are within the precision of the numerical method solution and make up no more than 1.66 % in the middle area of the plate. Thus, the developed mathematical model for the numerical solution of explosive loading allows to simulate the process of the Quardian 500 test plate explosive loading with high precision and can be used for estimation of landmine blast resistance of the KrAZ «Shrek» and KrAZ «Fiona» armored MPVs body.

**6.2. Simulation results.** The shape of the finite elements for the explosive charge, soil and air was generated automatically; for the vehicle body the shape of elements are tetrahedrons generated by the Patch Conforming algorithm. Parameters of the developed finite element model are given in Table 2. The general view of the simulation model with the explosive charge located under the left front wheel is shown in Fig. 2.

The explosive charge mass in the model was determined by changing the size and volume of the charge model. In the model the Flow Out boundary was used as the boundary condition. An additional condition in the form of gravitation, the vector of which is directed along the Z-axis and opposite to it, is also applied to the whole system (gravity accounting is important at the stage of calculation of soil emissions and movement of the body under the action of an explosive wave). To the lower edge of the V-shaped body bottom is also applied the restriction to the movement in the direction opposite to the Z-axis which is imitating the chassis on which the body is mounted, and prevents the body from falling down under the gravitation influence from the moment of the solving start.

The selective results of the simulation of KrAZ «Shrek» and KrAZ «Fiona» body explosive loading are presented on Fig. 7 and in Table 3.

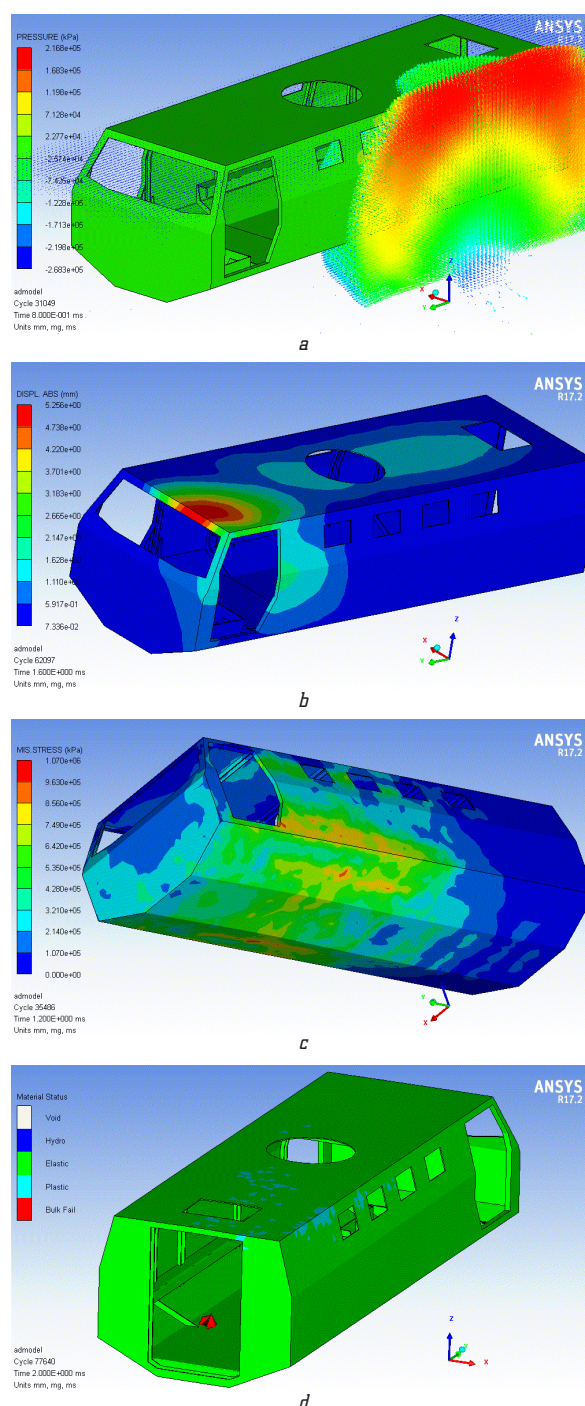


**Fig. 7.** Selective simulation results (charge mass and its location; time period after detonation): *a* – diagram of the explosive pressure distribution on the vehicle body (the shockwave is shown) (14 kg under left rear wheel; 0.8 ms); *b* – diagram of the body total deformations (10 kg under left front wheel; 1.6 ms); *c* – diagram of the equivalent (von Mises) stress on the vehicle body (20 kg under the vehicle center; 1.2 ms); *d* – destruction of the vehicle body (10 kg under left rear wheel; 2 ms)

Simulation model parameters

**Table 2**

| Object (material)           | Solver type | Overall dimensions |            |            | Mass-dimensional properties |          | FE-mesh parameters |          |
|-----------------------------|-------------|--------------------|------------|------------|-----------------------------|----------|--------------------|----------|
|                             |             | X-axis, mm         | Y-axis, mm | Z-axis, mm | volume, mm <sup>3</sup>     | mass, kg | nodes              | elements |
| Vehicle body (Quardian 500) | Lagrangian  | 2126               | 5876       | 1607       | 5.1861·10 <sup>9</sup>      | 4060.7   | 19329              | 58852    |
| Soil                        | Lagrangian  | 2304               | 7876       | 1000       | 1.8134·10 <sup>10</sup>     | 44247    | 1881               | 7848     |
| Air (atm.)                  | Eulerian    | 2304               | 7876       | 3011       | 5.4639·10 <sup>10</sup>     | 66.932   | 6840               | 5698     |



Table 3

The largest calculated deformations (mm) of the vehicles body and its condition

| Deformation zones | Level of threat according to NATO AEP-55 STANAG 4569 (charge mass) and its location |            |            |       |       |                 |            |            |       |       |             |            |            |       |       |
|-------------------|---|------------|------------|-------|-------|-----------------|------------|------------|-------|-------|-------------|------------|------------|-------|-------|
|                   | left front wheel  |            |            |       |       | left rear wheel |            |            |       |       | hull center |            |            |       |       |
|                   | II (6 kg)   | III (8 kg) | IV (10 kg) | 14 kg | 20 kg | II (6 kg)       | III (8 kg) | IV (10 kg) | 14 kg | 20 kg | II (6 kg)   | III (8 kg) | IV (10 kg) | 14 kg | 20 kg |
| L. board          | 1.58  | 2.23       | 3.11       | 6.45  | 7.80  | 2.37            | 13.5       | 22.9       | 9.70  | 12.2  | 9.27        | 11.1       | 13.6       | 14.3  | 19.9  |
| R. board          | 0.20  | 3.75       | 3.07       | 2.46  | 5.28  | 2.02            | 2.58       | 4.01       | 7.08  | 7.27  | 9.27        | 11.1       | 13.6       | 14.3  | 19.9  |
| Roof              | 4.16  | 7.26       | 9.32       | 16.7  | 19.4  | 10.2            | 28.1       | 30.1       | 27.5  | 34.7  | 2.29        | 5.01       | 4.49       | 5.12  | 29.9  |
| Bottom            | 0.95  | 1.38       | 1.63       | 2.80  | 3.47  | 2.67            | 3.06       | 15.4       | 10.2  | 14.6  | 13.5        | 17.7       | 24.3       | 25.3  | 46.7  |
| Destruction       | no  | no         | no         | no    | no    | no              | yes        | yes        | no    | yes   | no          | no         | no         | no    | no    |

**6.3. Results and research of the vehicles body destruction mechanism.** The theoretical assessment of the KrAZ «Shrek» and KrAZ «Fiona» vehicles landmine blast resistance allows to predict the destruction of the body in case of explosion of charge with mass of 8, 10 and 20 kg under the left rear wheel. On the Fig. 8 are shown the locations of the areas of destruction of the body relative to the points of initiation of detonation of the explosive.

However, the destruction does not occur in case of charge mass is 14 kg. The formation of irreversible plastic deformations in excess of the body material yield stress requires constant or increasing load for a certain time. As it can be seen from the systems of equations (9), (14) and expressions (10) and (12), such loads are possible provided in case the vector of the largest explosive wave pressure is located perpendicular to the loaded surface.

Also, let's note that the body moves under the influence of shockwave propagation. Given the scalar values of the body displacement velocity, the lateral surface of the body bottom constantly moves relative to the detonation point. Constructing a perpendicular from the body bottom to the detonation point, it is possible to see that the perpendicular constantly passing through the area of stress formation (as it shown on Fig. 9). The body material destruction is possible when its stress gradually begin to exceed the yield stress limit of the body material. Thus, the condition for the formation of the body irreversible deformations and its destruction is fulfilled.

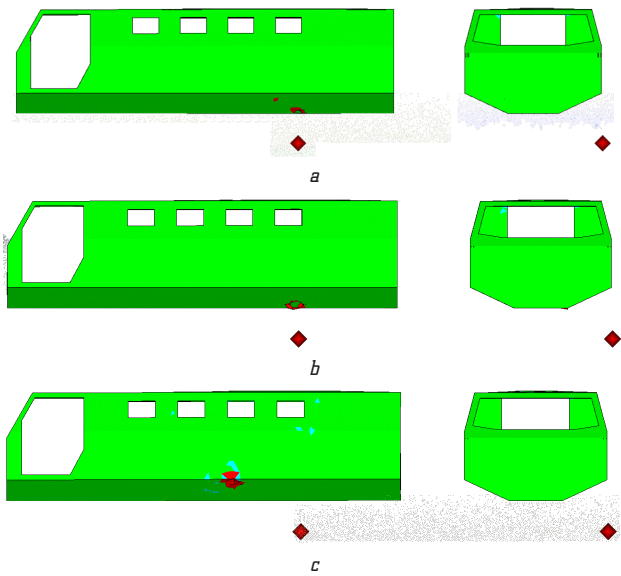


Fig. 8. Location of the areas of destruction of the body relative to the points of initiation of detonation of the explosive with mass in TNT equivalent: a – 8 kg; b – 10 kg; c – 20 kg

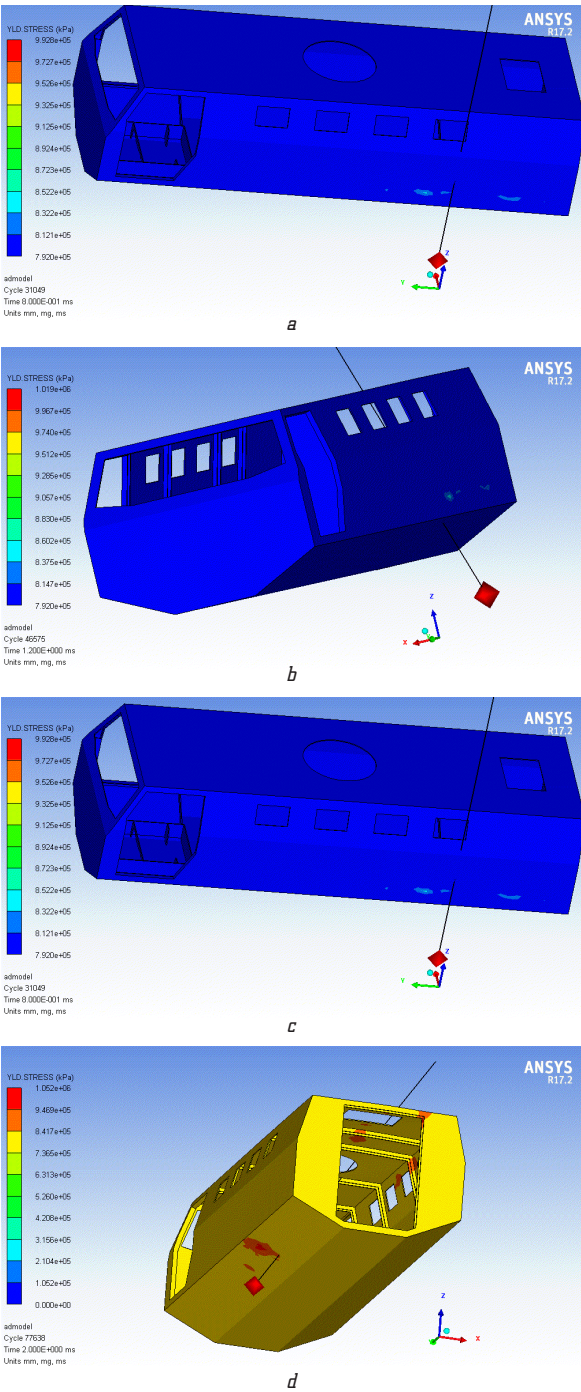


Fig. 9. The diagram of the vehicles body bottom yield stress at the detonation of explosive with a mass of 14 kg under the left rear wheel with the perpendicular built to the detonation point at the time after detonation: a – 1.033 ms; b – 1.2 ms; c – 1.6 ms; d – 2 ms

From the diagrams on Fig. 9 it is possible to see that in case of detonation of explosive with a mass of 14 kg at the time of 1.2 ms after detonation, the perpendicular passes almost past the lateral surface of the bottom. At a time of 1.6 ms, it passes through the lateral surface, in connection with which it creates an area of stress concentration; and in further it is shifting down and back. The maximum achieved stress reaches  $1.052 \cdot 10^6$  kPa (1052 MPa), which does not exceed the specified boundary of the material yield stress of 1200 MPa and is not sufficient for its destruction.

## 7. SWOT analysis of research results

**Strengths.** Comparison of the results of explosive loading of body material obtained by numerical and field experiments showed high reliability of the results obtained by modeling with Ansys AUTODYN software.

**Weaknesses.** Significant loads were obtained on the roof of the body and the side opposite the location of the explosive charge, which led to their bending outwards, due to leakage and propagation of the blast wave inside the body because the simplified body model did not take into account the presence of doors and glazing. The properties of sandy loam were set as a soil model. The calculation model did not take into account the structural elements of the explosive charge shell, and also used certain simplifications and assumptions.

**Opportunities.** It can be assumed that in the case of detonation of an explosive immersed in another type of soil with the different ability to absorbing or reflecting the blast wave and/or particles, the simulation results will differ from the accepted calculations. Also as in the case of taking into account the different designs of the body and vehicle or in case of inhomogeneity or inconsistency of body declared material properties, the results of the defeat of the vehicle body by the blast wave will be different from those obtained in this research.

**Threats.** Numerical analysis, as a rule, needs to be subdivided into problem domain analysis to the nodes, elements, and spatial discretization. The spatial discretization is performed by representing the fields and structures of the problem using computational points in space and connected with each other through a computational grid. Usually, the fine grid will lead to more accuracy of the result. The most popular spatial discretization has been widely used are Lagrange, Euler, ALE, and SPH and are provided in the AUTODYN computer code which usually shows acceptable simulation results.

However, it should be noted that mistakes in the generation of the mesh, as well as the simulation of complex objects, like the entire SPH method as a whole, requires significant computing power and can lead to critical errors associated with the energy balance such as critically small calculation time step or too large energy errors.

## 8. Conclusions

1. The mathematical model of pulse loading of armored steel Guardian 500 is developed. The process of deformation of body material in the conditions of difficult loading with the transition from the stationary center of deformation to nonstationary and force intensification is investigated.

The nature of the behavior of the shock wave formed as a result of the detonation of an explosive has been studied. Analytical dependences of the interaction of the shock wave with the loaded surface are made. A mathematical apparatus for calculating such parameters of the shockwave as the detonation front pressure and its change in time and the speed of the shockwave at the time of reaching the surface has been developed.

An experimental study of the dynamic explosive load of Guardian 500 steel and a comparison of the results with analytical calculations has been done. The adequacy of the developed mathematical model of numerical research of explosive loading to results of a full-scale experiment has been defined.

2. Theoretical calculation of mine resistance of KrAZ «Shrek» and KrAZ «Fiona» specialized armored vehicles bodies has been developed according to the requirements of the NATO standardization agreement AEP-55 STANAG 4569 – the detonation of explosive charge weighing 6, 8, and 10 kgs under each wheel and center of the vehicle and detonation of explosive charge weighing 14 and 20 kgs under each wheel and the center of the vehicle.

3. The conformity of landmine resistance of the KrAZ «Shrek» and KrAZ «Fiona» vehicles body to the requirements of STANAG 4569 – level II, levels 3b, 4b (completely), levels 3a, 4a (partially) has been established by numerical modeling. It has been established that the resistance of the body to the detonation of a charge weighing up to 20 kg, including the location of the charge under the front wheel and the center of the vehicles.

4. The conditions and mechanism of the KrAZ «Shrek» and KrAZ «Fiona» body destruction under pulse explosive loading have been investigated and theoretically substantiated. The destruction of the body during the detonation of an explosive charge weighing from 8 kg under the rear wheel has been studied.

## References

1. Gulzhan, A. K., Ursign, H., Yeonju, J., Pascal, R. (2018). *Global mapping and analysis of anti-vehicle mine incidents in 2017*. Geneva: GICHD–SIPRI. Available at: [https://www.sipri.org/sites/default/files/2018-05/global\\_mapping\\_and\\_analysis\\_of\\_anti-vehicle\\_mine\\_incidents\\_in\\_2017.pdf](https://www.sipri.org/sites/default/files/2018-05/global_mapping_and_analysis_of_anti-vehicle_mine_incidents_in_2017.pdf)
2. NATO AEP-55 STANAG 4569 – *Protection Levels for Occupants of Logistic and Light Armoured Vehicles*. Available at: <http://ballistics.com.au/technical/industry-ballistic-stab-resistant-standards/#stanag>
3. Trotsko, O., Shlyk, S. (2018). Development of the Sheet Blanks Forming Mathematical model for Calculation Using Simulation in ANSYS Software. *2018 IEEE International Scientific and Technical Conference on Computer Sciences and Information Technologies (CSIT)*, 169–172. doi: <http://doi.org/10.1109/stc-csit.2018.8526614>
4. Fiserova, D. (2006). *Numerical Analyses of Buried Mine Explosions with Emphasis on Effect of Soil Properties on Loading*. Cranfield. Available at: <https://dspace.lib.cranfield.ac.uk/bitstream/handle/1826/1209/darina%20fiserova.pdf>
5. Banadaki, M. M. D. (2010). *Stress-wave induced Fracture in Rock due to Explosive Action*. Toronto. Available at: [https://tspace.library.utoronto.ca/bitstream/1807/27567/1/Dehghan-Banadaki\\_Mahdi\\_201011\\_PhD\\_Thesis.pdf](https://tspace.library.utoronto.ca/bitstream/1807/27567/1/Dehghan-Banadaki_Mahdi_201011_PhD_Thesis.pdf)
6. Vorobyov, V., Pomazan, M., Shlyk, S., Vorobyova, L. (2017). Simulation of dynamic fracture of the borehole bottom taking into consideration stress concentrator. *Eastern-European Journal of Enterprise Technologies*, 3 (1 (87)), 53–62. doi: <http://doi.org/10.15587/1729-4061.2017.101444>
7. Laine, L., Ranestad, O., Sandvik, A., Snekkjevik, A. (2002). Numerical Simulation of Anti-Tank Mine Detonations. *Shock Compression of Condensed Matter*, 431–434. doi: <http://doi.org/10.1063/1.1483570>

8. Aubram, D., Rackwitz, F., Wriggers, P., Savidis, S. A. (2015). An ALE method for penetration into sand utilizing optimization-based mesh motion. *Computers and Geotechnics*, 65, 241–249. doi: <http://doi.org/10.1016/j.compgeo.2014.12.012>
9. Kurtoglu, I. (2017). A Review of S-ALE Solver for Blast Simulations. *11th European LS-DYNA Conference*. Available at: [https://www.researchgate.net/profile/Ilker-Kurtoglu/publication/320727967\\_A\\_Review\\_of\\_S-ALE\\_Solver\\_for\\_Blast\\_Simulations/links/59f80a9aa6fdcc075ec7cbd9/A-Review-of-S-ALE-Solver-for-Blast-Simulations.pdf](https://www.researchgate.net/profile/Ilker-Kurtoglu/publication/320727967_A_Review_of_S-ALE_Solver_for_Blast_Simulations/links/59f80a9aa6fdcc075ec7cbd9/A-Review-of-S-ALE-Solver-for-Blast-Simulations.pdf)
10. Dragobetskii, V., Shapoval, A., Mos'pan, D., Trotsko, O., Lotous, V. (2015). Excavator bucket teeth strengthening using a plastic explosive deformation. *Metallurgical and Mining Industry*, 4, 363–368.
11. Zaidi, A. M. A., Koslan, F. S., Othman, Z., Manar, G. (2013). Appropriate Coupling Solvers for the Numerical Simulation of Rolled Homogeneous Armor Plate Response Subjected to Blast Loading. *Advances in Mechanical Engineering*, 5, 637564. doi: <http://doi.org/10.1155/2013/637564>
12. Neuberger, A., Peles, S., Rittel, D. (2009). Springback of circular clamped armor steel plates subjected to spherical air-blast loading. *International Journal of Impact Engineering*, 36 (1), 53–60. doi: <http://doi.org/10.1016/j.ijimpeng.2008.04.008>
13. Laine, L., Sandvik, A. (2001). Derivation of mechanical properties for sand. *4th Asia-Pacific Conference on Shock and Impact Loads on Structures Singapore*, 361–368.
14. Dragobetskii, V., Shapoval, A., Naumova, O., Shlyk S., Mospan, D., Sikulskiy, V. (2017). The Technology of Production of a Copper – Aluminum – Copper Composite to Produce Current Lead Buses of the High – Voltage Plants. *IEEE International Conference on Modern Electrical and Energy Systems*, 400–403. doi: <http://doi.org/10.1109/mees.2017.8248944>
15. Dragobetskii, V., Zagirnyak, V., Shlyk, S., Shapoval, A., Naumova, O. (2019). Application of explosion treatment methods for production Items of powder materials. *Przegląd Elektrotechniczny*, 95 (5), 39–42.
16. Dragobetskii, V., Zagirnyak, M., Naumova, O., Shlyk, S., Shapoval, A. (2018). Method of Determination of Technological Durability of Plastically Deformed Sheet Parts of Vehicles. *International Journal of Engineering & Technology*, 7 (4.3), 92–99. doi: <http://doi.org/10.14419/ijet.v7i4.3.19558>

**Sergii Shlyk**, PhD, Associate Professor, Department of Manufacturing Engineering, Kremenchuk Mykhailo Ostrohradskyi National University, Kremenchuk, Ukraine, e-mail: [svshlyk@gmail.com](mailto:svshlyk@gmail.com), ORCID: <https://orcid.org/0000-0001-9422-1637>